Available online at www.sciencedirect.com
SCIENCE DIRECT®
Bioorganic & Medicinal Chemistry 12 (2004) 5225–5235
Bioorganic & Medicinal Chemistry

Analysis of human topoisomerase I inhibition and interaction with the cleavage site +1 deoxyguanosine, via in vitro experiments and molecular modeling studies

Gary S. Laco,[a] Wu Du,[b] Glenda Kohlhagen,[a] Jane M. Sayer,[c] Donald M. Jerina,[c] Thomas G. Burke,[d,e,✠] Dennis P. Curran[b] and Yves Pommier[a,*]

[a]*Laboratory of Molecular Pharmacology, Division of Basic Sciences, National Cancer Institute, National Institutes of Health, Bethesda, MD, 20892, USA*
[b]*University of Pittsburgh, Department of Chemistry, Pittsburgh, PA 15260, USA*
[c]*Laboratory of Bioorganic Chemistry, National Institute of Diabetes and Digestive and Kidney Diseases, National Institutes of Health, Bethesda, MD, 20892, USA*
[d]*Division of Pharmaceutics Sciences, College of Pharmacy and Experimental Therapeutics Program, Markey Cancer Center, University of Kentucky, Lexington, KY 40506, USA*
[e]*Tigen Pharmaceuticals, Inc., Lexington, KY 40506, USA*

Received 9 April 2004; accepted 9 June 2004
Available online 11 August 2004

Abstract—Human topoisomerase I (Top1) plays a pivotal role in cell replication and transcription, and therefore is an important anti-cancer target. Homocamptothecin is a lead compound for inhibiting Top1, and is composed of five conjugated planar rings (A–E). The homocamptothecin E-ring β-hydroxylactone opens slowly to a carboxylate at pH > 7.0. We analyzed, which form of homocamptothecin was biochemically relevant in the following ways: (1) the homocamptothecin carboxylate was tested for activity in vitro and found to be inactive; (2) homocamptothecin was incubated with Top1 and dsDNA, and we found that the homocamptothecin β-hydroxylactone form was stabilized; (3) the homocamptothecin E-ring β-hydroxylactone was modified to prevent opening, and the derivatives were either inactive or had low activity. These results indicated that the homocamptothecin β-hydroxylactone was the active form, and that an E-ring carbonyl oxygen and adjacent unsubstituted/unprotonated ring atom were required for full activity. Homocamptothecin and derivatives were docked into a Top1/DNA active site model, in which the +1 deoxyguanosine was rotated out of the helix, in order to compare the interaction energies between the ligands and the Top1/DNA active site with the in vitro activities of the ligands. It was found that the ligand interaction energies and in vitro activities were correlated, while the orientations of the ligands in the Top1/DNA active site explained the importance of the E-ring β-hydroxylactone independently of E-ring opening. An essential component of this Top1/DNA active site model is the rotated +1 deoxyguanosine, and in vitro experiments and molecular modeling studies supported rotation of the +1 deoxyguanosine out of the helix. These results allow for the rational design of more potent Top1 inhibitors through engineered interactions with as yet unutilized Top1 active-site residues including: Glu356, Asn430, and Lys751.

1. Introduction

Human topoisomerase 1 (Top1) relaxes supercoiled DNA and so allows for cellular replication and transcription.[1–3] This key role of Top1 has made it an anti-cancer target, and several reviews have compiled the numerous Top1 inhibitors that have been isolated, synthesized, and evaluated in vitro and in vivo.[4,5] Camptothecin (CPT, Table 1) is a Top1 inhibitor that was first isolated from the Chinese tree *Camptotheca acuminata*.[6] CPT is the lead compound for derivatives

Abbreviations: Top1, human topoisomerase I; HCPT, homocamptothecin; CPT, camptothecin; dsDNA, double-stranded DNA; ssDNA, single-stranded DNA; dG, deoxyguanosine.

Keywords: Human topoisomerase I; Homocamptothecin E-ring lactone; Rotated +1 dG.

* Corresponding author. Tel.: +1-301-496-5944; fax: +1-301-402-0752; e-mail: pommier@nih.gov
✠ Deceased.

0968-0896/$ - see front matter © 2004 Elsevier Ltd. All rights reserved.
doi:10.1016/j.bmc.2004.06.046

Table 1. hCPT E-ring lability and inhibition of Top1 by CPT/hCPT and derivatives

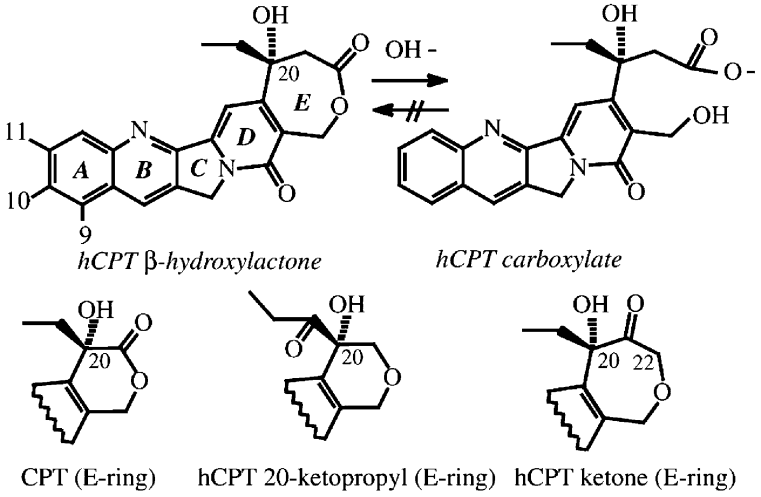

Ligand	Relative inhibition of Top1	A-ring position		
		9	10	11
CPT	0.9	H	H	H
hCPT	1.0	H	H	H
hCPT 20-ketopropyl[a]	O.1	H	H	H
hCPT ketone[a]	N.D.	H	H	H
hCPT 9.10 diF	10.5	*F*	*F*	H
hCPT 10,11 diF	12.0	H	*F*	*F*

N.D., not detected.
[a] Racemic ligands.

that have resulted in more potent Top1 inhibitors and these have been discussed in several reviews.[5,7]

Mechanistically, Top1 attacks the backbone phosphate of supercoiled DNA with the active-site Tyr723. This results in a tyrosyl-phosphate bond between Tyr723 and the 3′ end of the −1 cleavage-site deoxynucleoside, and a free 5′-OH on the +1 cleavage-site deoxynucleoside (+1 deoxynucleoside).[8–10] We have previously proposed that Top1 then rotates the +1 deoxynucleoside with its free 5′-OH out of the helix to prevent premature religation of partially relaxed DNA,[11,12] thus making Top1 a processive enzyme.[13] After the DNA is fully relaxed, rotation of the +1 deoxynucleoside back into the helix would then be favored to allow both religation of the DNA and for Top1 to bind another supercoiled DNA.[12] Here we experimentally tested whether the +1 deoxyguanosine (dG) rotated out of the helix when Top1 was trapped in covalent complex with DNA by an inhibitor, and then computationally analyzed the interactions between the +1 dG and Top1.

Religation is inhibited by CPT and its active derivatives.[3,14] In the above model, CPT binds in the Top1/DNA active site such that it blocks the rotated +1 deoxynucleoside from re-entering the helix and so traps Top1 in covalent complex with DNA.[12] In the cell, CPT-stabilized Top1/DNA covalent complexes generate double-strand DNA (dsDNA) breaks after collision with replication complexes,[15–17] and these dsDNA breaks in the cell are thought to trigger a cytotoxic cascade that results in cell death.[18–20] In this way actively dividing cells, such as cancer cells, can be targeted by CPT and derivatives. CPT-resistant cells have been selected for in cell culture, while molecular modeling studies have been used to engineer Top1 resistance to 10-OH derivatives of CPT.[12] To date over 10 Top1 mutations resulting in resistance to CPT and 10-OH derivatives have been identified.[5,12] The Top1 resistance mutations cluster predominately around the +1 base pairs in the Top1/DNA active site.[5]

An important problem with CPT is that the electrophilic six-member E-ring can readily open to a carboxylate at pH > 7.0.[21,22] There have been conflicting reports as to whether or not CPT carboxylate inhibits Top1. While Hertzberg et al.[23] reported that the CPT α-hydroxylactone and carboxylate had equal activities in vitro, another study reported that the CPT carboxylate had significantly lower activity in vitro.[24] These divergent results may be due to the reversibility of the CPT E-ring carboxylate to the α-hydroxylactone during the assay.[25] When the α-hydroxylactone forms of soluble CPT derivatives were added to human plasma, the E-ring opened and the resulting carboxylate form was bound by serum albumin.[21,26,27] This drove the equilibrium toward the carboxylate form, and resulted in the rapid clearance of CPT α-hydroxylactone from the blood with a half-life of approximately 21 min.[21] In order to stabilize the CPT E-ring, a seven-member E-ring derivative of CPT was synthesized and named homocamptothecin (hCPT, BN 80245,[28] Table 1). The hCPT β-hydroxylactone E-ring

exhibited significantly slower opening than the CPT E-ring in vitro, while at the same time hCPT demonstrated increased inhibition of Top1 in cell culture assays.[28] This raised the question as to whether a labile E-ring was essential for CPT and hCPT activity against Top1. Interestingly, while the hCPT E-ring does slowly open at pH > 7, this is an irreversible reaction.[28] In contrast to the inconclusive tests due to the reversibility of the CPT carboxylate (see above), conclusive testing can be done to determine whether the hCPT carboxylate form is active.

We used several approaches to examine the role of the hCPT E-ring lactone in inhibition of Top1: (1) We determined experimentally that the hCPT carboxylate was inactive in vitro and that the hCPT β-hydroxylactone was stabilized in the presence of Top1 and dsDNA. (2) We investigated a structural isomer of hCPT in which the hCPT E-ring β-hydroxylactone was reorganized as a ketone to prohibit E-ring opening (hCPT ketone, see Table 1). In addition, a hCPT derivative containing a six-member E-ring was made in which opening of the ring was also blocked (Table 1; hCPT 20-ketopropyl). (3) To gain insight into the activity of hCPT and the inactivity of the hCPT ketone derivative, the closed E-ring forms of all ligands were docked into a Top1/DNA active-site model. This allowed for the comparison of the ligands interaction energies with the Top1/DNA active site, with their respective in vitro activities.

2. Results and discussion

2.1. In vitro activities of hCPT and derivatives

hCPT, the fluorinated derivatives hCPT 9,10 diF (28a[29]), hCPT 10,11 diF (BN80195,[28] 28b[29]) and the hCPT ketone and hCPT 20-ketopropyl derivatives (Table 1, Du1441 and Du1442[30]) were tested for their ability to block Top1 religation of bound DNA in vitro. Ligands were incubated at concentrations from 0.01 to 10 μM with Top1 and an end-labeled dsDNA containing a single high-affinity −1T/+1G Top1 cleavage site (Fig. 1A, see Experimental). Top1 DNA cleavage products were separated by electrophoresis (Fig. 1B) and quantified (Table 1, CPT, hCPT, hCPT 20-ketopropyl were quantified at 10 μM, while hCPT 9,10 diF and hCPT 10,11 diF were quantified at 1 μM). The results shown in Figure 1B indicated that CPT and hCPT had similar activities in this assay. The fluorinated hCPT derivatives hCPT 9,10 diF and hCPT 10,11 diF were ~11-fold more potent than hCPT in inhibiting Top1 religation (Table 1). Fluorines can make H-bonds, and the F–H contact strength has been estimated to be up to 4 kcal/mol,[31] versus oxygen H-bonds, which have an O–H contact strength between 5 and 10 kcal/mol.[32] The increase in the activity of hCPT 9,10 diF and hCPT 10,11 diF suggested that the A-ring fluorines were within H-bonding distance of an H-bond donor in the Top1/DNA active site. In contrast, hCPT ketone does not have detectable activity against Top1 (Fig. 1B), while hCPT 20-ketopropyl had low activity against Top1 (Fig. 1B, Table 1).

2.2. hCPT E-ring opening

One possible explanation for the lack of activity of hCPT ketone and hCPT 20-ketopropyl is that their E-rings cannot open to a carboxylate. Exogenously supplied hCPT carboxylate is inactive (Fig. 1B). However, it is possible that the carboxylate form of hCPT is active only when formed in situ in the Top1/DNA active site. To test this possibility, hCPT E-ring opening was analyzed in the presence of buffer (pH 10.5 and 7.4), and Top1 and dsDNA (Fig. 2, see Experimental). At pH 10.5 the hCPT E-ring opened quantitatively (Fig. 2B) while at pH 7.4 only 4.4% of the carboxylate form

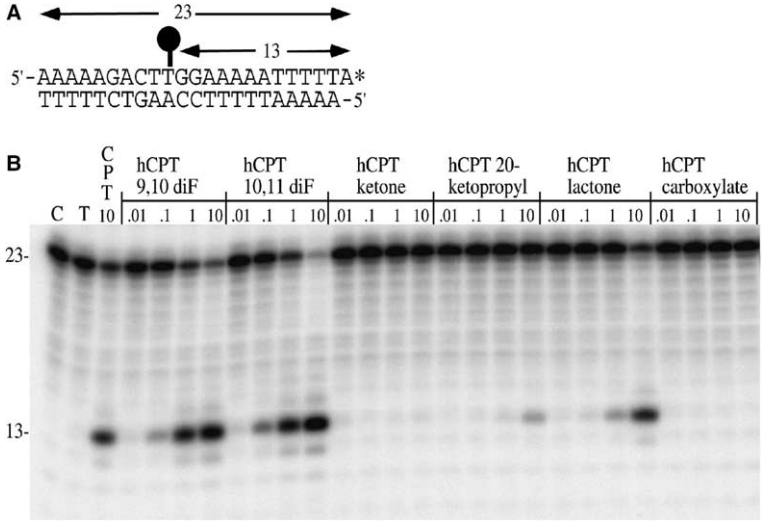

Figure 1. In vitro inhibition of Top1 by hCPT and derivatives. (A) Schematic diagram of the 3′-labeled 23-mer dsDNA substrate (the ^{32}P-cordycepin label is indicated by ∗), with Top1 (black circle) making a covalent bond to the DNA backbone resulting in the 13-mer cleavage product. (B) Top1 oligo assay for CPT, hCPT and derivatives. Reaction products were separated in denaturing PAGE. Lanes: C, control reaction with no added Top1; T, reaction with Top1 and oligo, but no inhibitor. All ligand concentrations are in μM. The 23-mer oligo is indicated on the left, as is the 13-mer cleavage product.

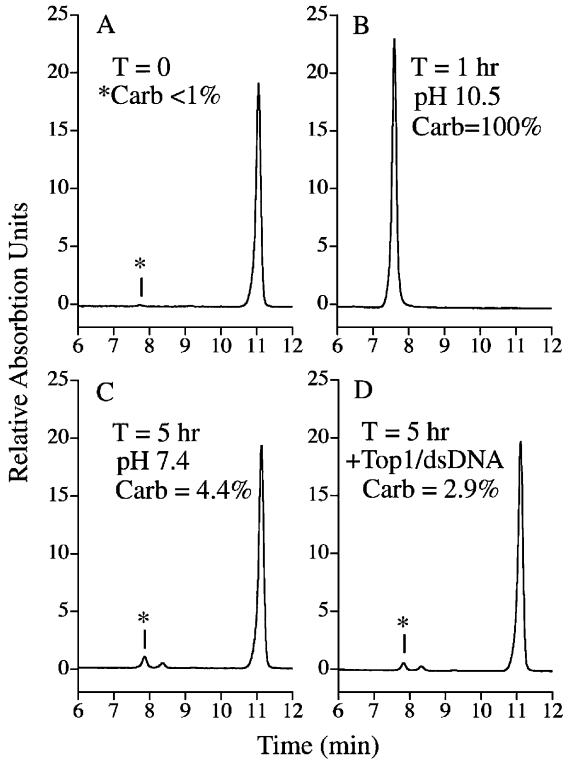

Figure 2. Analysis of hCPT E-ring opening in the absence or presence of Top1 and dsDNA. The hCPT β-hydroxylactone and carboxylate (Carb) forms were separated by HPLC (detection at 367 nm) and eluted at 11.2 and 7.8 min, respectively (see Experimental). (A) hCPT T = 0 control; (B) hCPT pH 10.5 buffer T = 1 h; (C) hCPT pH 7.4 buffer, T = 5 h; and (D) hCPT pH 7.4 buffer plus Top1 and dsDNA, T = 5 h. The percentages of hCPT carboxylate (Carb) are given. The hCPT lactone peak in A is less than the hCPT carboxylate peak in B, due to the difference in their respective extinction coefficients.

accumulated over 5 h (Fig. 2C), consistent with previously published data.[28] Interestingly, in the presence of Top1 and dsDNA only 2.9% of the hCPT E-ring opened (Fig. 2D; Top1/dsDNA:hCPT ratio of 2:1), and this result is consistently less than the buffer control (Fig. 2). Thus, Top1 and dsDNA do not catalyze E-ring opening of hCPT. These results are unambiguous because once the hCPT E-ring opens, it cannot close.[28] In addition, equal amounts of total hCPT (β-hydroxylactone and carboxylate) were recovered from the reactions regardless of whether they contained only buffer or in addition Top1 and dsDNA (Fig. 2), demonstrating that hCPT did not co-precipitate with Top1 and dsDNA in the methanol precipitation step (see Experimental). Since the carboxylate form of hCPT was inactive (Fig. 1B), and hCPT E-ring opening was suppressed in the presence of Top1 and dsDNA (Fig. 2D), we concluded that the E-ring opened form of hCPT does not inhibit Top1. Thus, only the lactone forms of CPT, hCPT and derivatives were used in the molecular modeling studies.

2.3. Top1 interaction with the +1 dG in vitro and via molecular modeling studies

An essential component of this Top1/DNA active site model is the rotated +1 dG.[11,12] Here we analyzed the interaction of the Top1/DNA active site with the +1 dG in vitro. hCPT was used to trap Top1 in covalent complex with dsDNA, and then $CoCl_2$ was used to generate sulfate radicals from $KHSO_5$ (see Experimental). The sulfate radicals specifically oxidize extra-helical guanines.[33,34] The oxidation reaction was allowed to proceed for 5 min and then stopped with EDTA. Piperidine was then used to cleave the backbone of the DNA 3′ to the oxidized guanines, leaving a 5′ phosphate.[33] The reaction products were then separated by 20% PAGE with 7 M urea. In Figure 3 lane 4, the +1 dG in the hCPT trapped Top1/DNA cleavage complex was oxidized and cleaved off to give a 22-mer product with a 5′ phosphate (Fig. 3). In the presence of Top1 and dsDNA (Fig. 3, lanes 6) a modest amount of oxidation specific for the +1 dG occurred, while in the absence of active Top1 (Fig. 3, lanes 7–8) there was minimal oxidation of dG's with no selectivity for the +1 dG. The use of PAGE purified oligonucleotides in this assay eliminated the nonspecific background bands seen in Figure 1B (see Experimental).

In order to determine if the rotated +1 dG made favorable interactions with the solvated Top1/DNA active site,

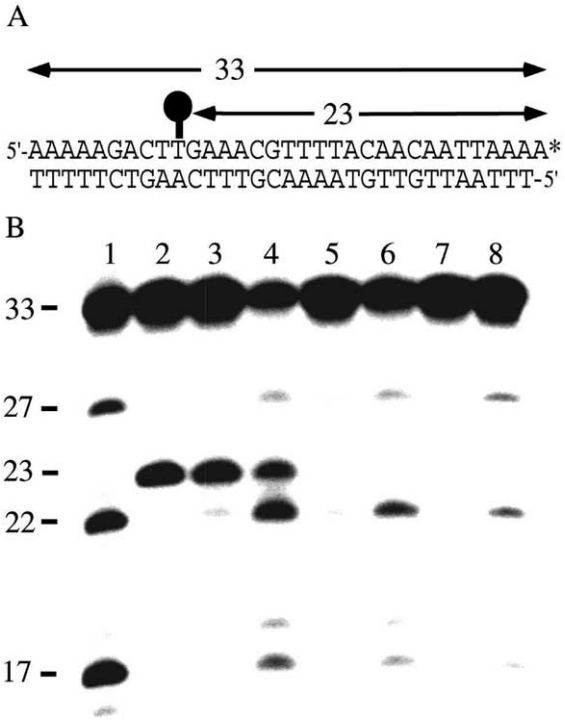

Figure 3. Oxidation of rotated deoxyguanosines followed by cleavage of the DNA backbone 3′ to the oxidized deoxyguanosine by piperidine (see Experimental). Lane 1, oxidized ssDNA (800 μM $CoCl_2$ and 10-fold excess of $KHSO_5$) followed by treated with piperidine; Lane 2, Top1, dsDNA and hCPT were incubated for 15 min and then treated with piperidine (no oxidation step); Lanes 3–4, Top1, dsDNA and hCPT were incubated for 15 min, oxidized (200 and 800 μM $CoCl_2$ and 10-fold excess of $KHSO_5$, respectively) and then treated with piperidine; Lanes 5–6, Top1 and dsDNA were incubated for 15 min, oxidized (200 and 800 μM $CoCl_2$ and 10-fold excess of $KHSO_5$, respectively) and then treated with piperidine; Lanes 7–8, dsDNA was incubated for 15 min, oxidized (200 and 800 μM $CoCl_2$ and 10-fold excess of $KHSO_5$, respectively) and then treated with piperidine.

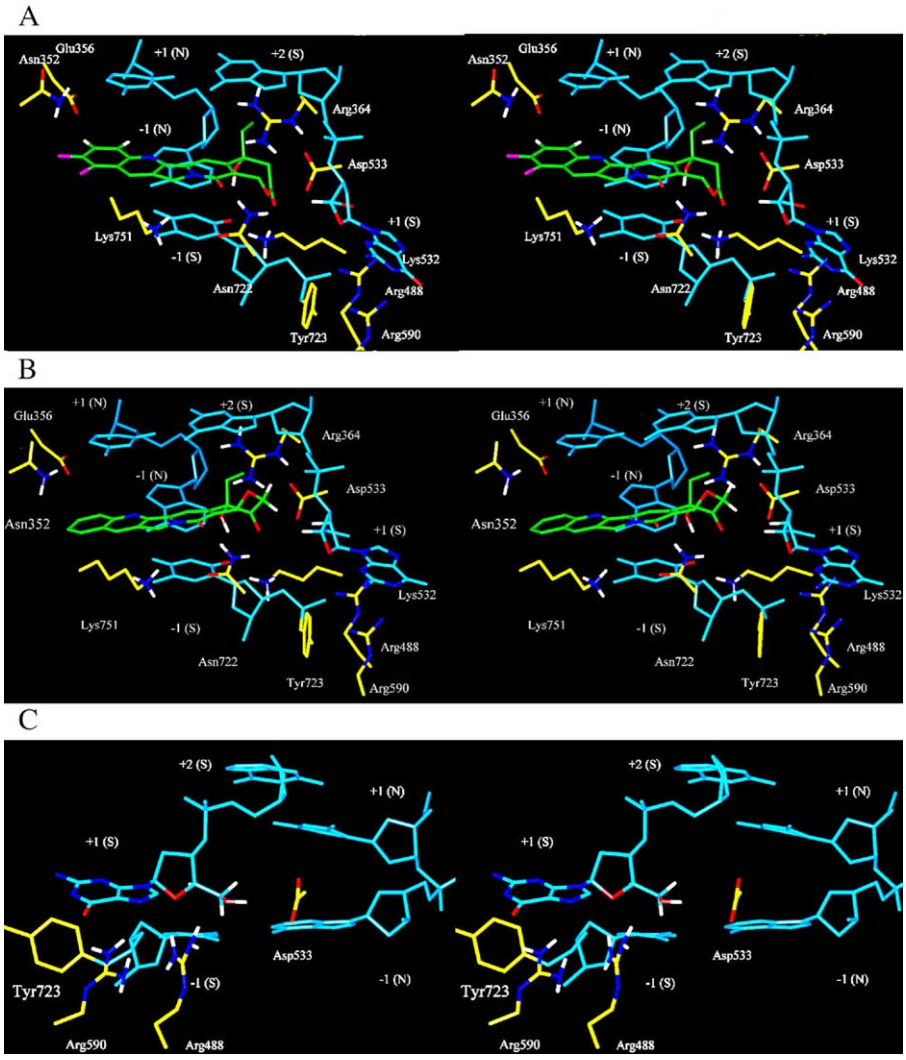

Figure 4. Stereo view of ligands (A, B) and the rotated +1 dG (C) in the Top1/DNA active site. For A and B the view is looking toward the major groove of the DNA, down the main axis of Tyr723. DNA is light blue, amino acid side chains are yellow, nitrogens are blue, oxygens are red, and hydrogens are white (for clarity, only selected hydrogens are shown, and waters and counter ions are not shown). Note that the +1 dG has been rotated out of the DNA helix. The Top1 active-site Tyr723 is covalently linked to the −1 thymine. Scissile-strand bases indicated by (S), while the nonscissile-strand bases are indicated by (N). (A) hCPT 9,10 diF is green and fluorines are magenta, A ring to the left, E ring to the right. Hydrogens are shown only on the A-ring and the E-ring 20-OH. (B) hCPT ketone is green, hydrogens are shown only on the A-ring, the 20-OH, and the E-ring ketone. (C) The orientation in A was rotated ~90° to the left. View from the minor groove, perpendicular to the main axis of Tyr723, showing the rotated +1 dG and Top1 residues Arg488, Asp533, and Arg590. Bases are labeled as in A and B.

the solvent, rotated +1 dG, and the following Top1 residues were minimized: Arg488, Asp533, Ile535, and Arg590. After minimization, it was found that Arg590 makes H-bonds/electrostatic interactions with the +1 dG carbonyl oxygen and ring nitrogen (N7), while Arg488 makes H-bonds to the ribose ring oxygen and the 5′-OH oxygen (Figs. 4C and 5B). The +1 dG 5′-OH hydrogen also makes an electrostatic interaction with Asp533 (Fig. 5B). In addition, Asp533 acts as a doorstop by preventing the +1 dG from rotating further out of the helix and in so doing aligns it for optimal interactions with Arg488 and Arg590 (Fig. 4C). The interaction energy between the rotated +1 dG and Top1 is −180.05 kcal/mol (van der Waals −28.25 kcal/mol, electrostatic −151.80 kcal/mol). The dominant electrostatic component of this interaction energy is consistent with the salt reversibility of CPT trapped Top1/DNA covalent complexes.[35]

2.4. Ligand interactions with the solvated Top1/DNA active site

Analysis of the minimized hCPT 9,10 diF Top1/DNA active site in Figure 4A (see Experimental) revealed that the hCPT 9,10 diF orientation in the active site cavity was perpendicular to the main axis of the DNA, parallel to the bases, and projected outward from the major groove (Fig. 4A; hCPT adopts a similar orientation, data not shown). The hCPT 9,10 diF D-ring stacks on top of the scissile-strand −1 thymine, the E-ring 20-ethyl projects underneath the scissile-strand +2 guanine (in the space vacated by the rotated +1 dG), while the A-ring 10-F approaches Asn352. Interestingly, the current model is consistent with the strong hCPT preference for a +1 dG.[36] The rotated +1 dG leaves a cavity within the helix that the hCPT 9,10 diF E-ring 20-ethyl fills in this model (Fig. 4A). A +1 dC would leave a smaller cavity,

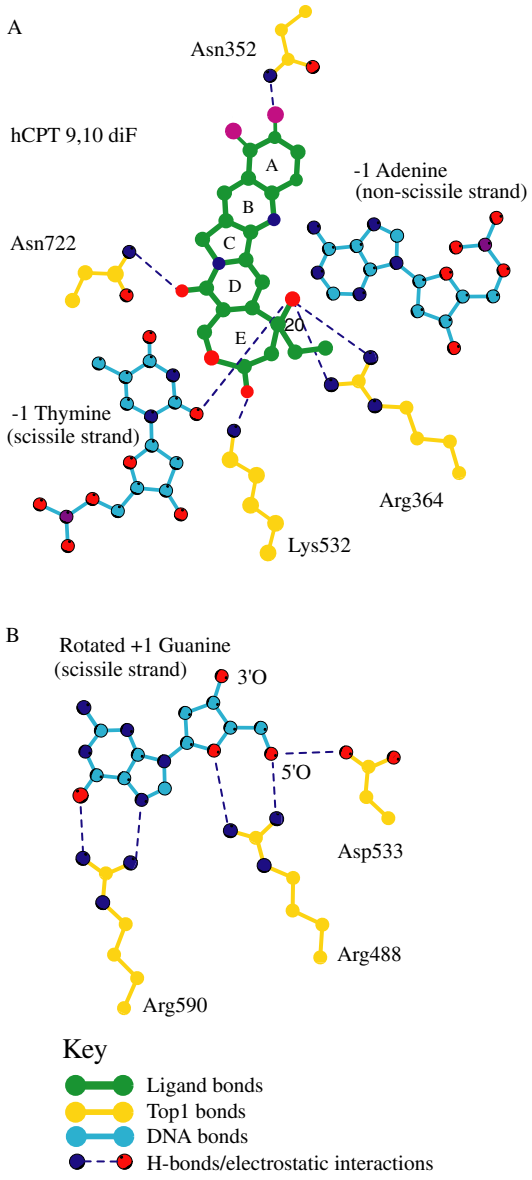

Figure 5. Flattened views of Figure 3A and C showing H-bonds/electrostatic interactions. (A) hCPT 9,10 diF is green and H-bonds/electrostatic interactions with Top1 residues and bound DNA are indicated by dashed lines. (B) The H-bonds/electrostatic interactions between the rotated +1 dG and Top1 residues are indicated by dashed lines. Hydrogens are not shown.

and the complementary nonscissile-strand +1 dG would then make a steric clash with the E-ring 20-ethyl (data not shown).

H-bonds/electrostatic interactions between hCPT 9,10 diF and the Top1/DNA active site include the following: (1) the E-ring carbonyl oxygen makes a H-bond with Lys532 an essential residue[37] (Fig. 5A, Insight II H-bond parameters), and this is the dominant electrostatic interaction between hCPT 9,10 diF and Top1; (2) the D-ring carbonyl oxygen makes a H-bond to Asn722, that when mutated to Ser results in Top1 resistance to CPT.[38] Removal of the D-ring carbonyl oxygen resulted in an inactive CPT derivative;[39] (3) the E-ring 20-OH oxygen makes an electrostatic interaction with Arg364 (~4 Å). Mutation of Arg364 to His resulted in Top1/Arg364His resistance to CPT.[40] The electrostatic interaction between the E-ring 20-OH and Arg364 is consistent with the mutability of the 20-OH to unprotonated electronegative atoms (i.e., Cl, Br) while retaining a fraction of the original activity;[41] (4) the E-ring 20-OH hydrogen makes a H-bond to the scissile-strand −1 thymine carbonyl oxygen, and the loss of this H-bond by CPT 20-Cl/Br derivatives is likely responsible for the reduction in their activities.[41] The hCPT 9,10 diF A-ring 10-F accepts a H-bond from the Asn352 nitrogen, while the adjacent A-ring 11-H makes a weak electrostatic interaction with the exposed Asn352 nitrogen. In contrast, when hCPT 10,11 diF is in the same orientation the A-ring 10-F H-bonds to Asn352 while the 11-F makes a repulsive interaction with the exposed Asn352 nitrogen. The repulsive interaction between the A-ring 11-F and Asn352 resulted in the Asn352 NH_2 rotating during the minimization until it became perpendicular to the plane of the A-ring. This allowed Asn352 to avoid a repulsive electrostatic interaction with the hCPT 10,11 diF A-ring 11-F while still H-bonding to the adjacent 10-F (data not shown). Mutation of Asn352 to Ala results in a Top1 that is inhibited to the same extent by CPT as by the more potent 10-OH derivatives.[12] The flexibility of Asn352 during molecular dynamics simulations of a Top1/DNA complex[42] supports it being allowed to adopt the different orientations presented here.

2.5. Interaction energies between ligands and the solvated Top1/DNA complex

In order to see if the binding orientations of the ligands correlated with their in vitro activities, the nonbond interaction energies between all the minimized ligand/Top1/DNA complexes were calculated (Table 2, see Experimental). While CPT has similar in vitro activity as hCPT (Table 1), it does have a weaker van der Waals interaction energy than hCPT. This can be attributed to the smaller and less bent CPT E-ring and consequently reduced surface contact area with the scissile-strand −1 thymine and the rotated +1 dG ribose (data not shown). The larger and more bent hCPT E-ring's increased van der Waals interaction with the active site, including the rotated +1 dG ribose, may contribute to its greater resistance to the use of salt to force it out of the Top1/DNA active site (Fig. 4A), versus CPT.[36] The hCPT 20-ketopropyl (in which the E-ring cannot open) was docked in the same orientation as hCPT; however, it had low activity against Top1 (Table 1) and a 3.7 kcal/mol weaker electrostatic interaction energy (Table 2). This is consistent with the hCPT 20-ketopropyl not having an E-ring carbonyl oxygen that can H-bond to Lys532 (see Table 1). The stronger hCPT 20-ketopropyl van der Waals interaction energy can be attributed to the increased contact the extended E-ring 20-ketopropyl makes with the +2 scissile-strand adenine and Arg364 (as compared to the shorter and more angular CPT 20-ethyl, data not shown). The inactive hCPT ketone derivative, like the hCPT 20-ketopropyl, also has a significant loss in electrostatic energy versus hCPT (5.8 kcal/mol, Table 2), even though the hCPT ketone has an E-ring carbonyl oxygen that is in an orientation

Table 2. Interaction energies between ligands and the Top1/DNA complex

Ligands	van der Waals	Electrostatic	Total energy
CPT	−55.83[a]	−31.68	−87.51
hCPT	−58.01	−30.29	−88.30
hCPT 20-ketopropyl	−56.35	−26.60	−82.95
hCPT ketone	−57.12	−24.44	−81.56
hCPT 9,10 diF	−58.65	−34.89	−93.54
hCPT 10,11 diF	−59.29	−32.79	−92.08

[a] kcal/mol.

similar to the E-ring carbonyl oxygen of CPT (Table 1). This lack of activity by the hCPT ketone can be explained by the E-ring C22 hydrogen's (Table 1) making a repulsive van der Waals interaction with the rotated +1 dG ribose hydrogen's that force the hCPT ketone to move toward/under Asn352 (Fig. 4B). The net result is the loss of the H-bond between the hCPT ketone E-ring carbonyl oxygen and Lys532, loss of the electrostatic interaction between the E-ring oxygen and Lys532 (since it is replaced by a methylene group; see Table 1), reduction in the van der Waals/electrostatic interactions with Arg364 and Asn722, and reduction in the E-ring van der Waals interaction with the +1 rotated dG ribose. The fluorinated derivatives hCPT 9,10 diF and hCPT 10,11 diF have significantly stronger electrostatic interaction energies than hCPT (Table 2), and this correlates with their respective A-ring 10-F H-bonding to Asn352 (Figs. 4A and 5A).

3. Conclusions

In the battle against cancer, Top1 is a key target because of its pivotal role during cellular transcription and replication.[1–3] hCPT is a lead compound for the development of more potent Top1 inhibitors. In order to gain insight into the structure–activity relationship of hCPT and derivatives we used in vitro assays as well as computational analyses of the ligands' interaction with a solvated Top1/DNA active-site model. Our results shows a strong correlation between the in vitro activities of Top1 inhibitors and their interaction energies with the Top1/DNA covalent complex, with electrostatic interactions playing a defining role in ligand activity.

Here we demonstrated that the hCPT carboxylate was inactive in vitro (Fig. 1B). In addition, hCPT E-ring opening was suppressed in the presence of Top1 and dsDNA (Fig. 2D). These results indicated that the carboxylate form of hCPT was not involved in inhibiting Top1. The in vitro oxidation results for the cleavage site +1 dG indicated that it rotated out of the helix when hCPT trapped Top1 in covalent complex with dsDNA, and this gives experimental support to a key part of our Top1/DNA active-site model.[11,12] The presence of a 22-mer oxidation product with only Top1 and dsDNA (Fig. 3B, lane 6), indicates that Top1 bound the dsDNA and rotated the +1 dG out of the helix, at which time it was oxidized. Since the dsDNA was fully relaxed, Top1 immediately rotated the oxidized +1 dG back into the helix and religated the DNA without making a stable Top1/DNA covalent complex and corresponding 23-mer cleavage product (Fig. 3B). A 7,8-dihydro-8-oxoguanine (an oxidized dG) at the +1 cleavage site did not prevent cleavage and religation of the dsDNA by Top1.[43] Since Top1 has a low affinity for relaxed dsDNA it may be difficult to visualize, by X-ray crystallography, Top1 in covalent complex with native dsDNA in which the rotated +1 dG makes a stable interaction with Top1 residues: Arg488, Asp533, and Arg590.

Computational analysis of the rotated +1 dG's interaction with Top1 revealed a network of H-bond/electrostatic interactions between it and Arg488, Asp533, and Arg590 (Fig. 5B, see Results and discussion). Interestingly, Arg590 makes a guanine specific contact with the rotated +1 dG (Fig. 5B), and this is consistent with the majority of Top1 cleavage sites containing a +1 guanine.[36] It has been proposed that one role of Asp533 is to hold the +1 dG out of the helix to prevent premature religation of the supercoiled DNA backbone, and so allow Top1 to fully relax the DNA.[11,12] Mutation of Asp533 to Gly results in a Top1, which has a 10-fold higher religation rate[13] and is resistant to CPT.[44] The increased religation rate of Top1 Asp533Gly can be explained by the loss in the stabilization of the rotated +1 dG by Asp533, thus allowing it to re-enter the helix and religate the DNA backbone more readily. Similarly, the CPT resistance of Top1 Asp533Gly can be attributed to a +1 dG that more freely rotates back into the helix, thus blocking entry of CPT into the Top1/DNA active site.

Analysis of the hCPT 20-ketopropyl derivative in vitro (Fig. 1) and its interaction energy score with the Top1/DNA active site (Table 2) indicates that the significant reduction in activity was due to the loss of the hCPT E-ring carbonyl oxygen's electrostatic interaction with Lys532 (see Results and discussion). In addition, the disruption of the hCPT E-ring β-hydroxylactone via the hCPT ketone derivative (Table 1) resulted in the loss of detectable activity in vitro (Fig. 1B). Based on our model, the lack of activity by the hCPT ketone is due to the E-ring C22 hydrogen's that make a steric clash with the rotated +1 dG ribose hydrogen's (Fig. 4B, see Results and discussion). This result also explains the inactivity of the CPT lactam derivative in which the E-ring lactone ring oxygen is replaced with a protonated nitrogen,[23] in that the E-ring nitrogen's hydrogen would also make a steric clash with the rotated +1 dG ribose's hydrogens forcing the CPT lactam away from Lys532, Asn722, and Arg364 (data not shown). Removal of the CPT E-ring oxygen to give a five-member E-ring

derivative with a carbonyl oxygen also resulted in an inactive compound, though the addition of electronegative atoms to the A-ring can restore a significant amount of activity,[45] Replacement of the CPT E-ring lactone carbon and ring oxygen with two methylene groups also resulted in a compound that had diminished activity against Top1 in an oligonucleotide assay and no detectable activity in a supercoiled DNA assay.[46] The above derivatives indicate the importance of the E-ring carbonyl oxygen with an adjacent unsubstituted/unprotonated ring atom for 'full activity' of CPT and hCPT. Such an atomic arrangement gives a lactone that is by nature labile, and so unavoidably results in the generation of the inactive CPT/hCPT carboxylate at pH 7 and above (Figs. 1B and 2C).

In the Top1/DNA active-site model presented here the orientation of hCPT explains the Top1 Asn352Ala, Arg364His, and Asn722Ser CPT and 10-OH CPT resistance mutations, via the loss of direct electrostatic interactions between the resistant Top1 mutants and CPT. These three Top1 residues form a triangle that is co-planar with the cleavage site +1 bases,[10] and hCPT 9,10 diF can contact the three Top1 residues in only two orientations: (1) with the 20-ethyl up and the E-ring carbonyl oxygen pointing down toward Lys532 (Fig. 4A); or (2) with the 20-ethyl down and the E-ring carbonyl oxygen pointing up toward the solvent (data not shown). Only with hCPT 9,10 diF orientated as in 1 (see Fig. 4A) can the importance of the E-ring carbonyl oxygen be explained via its H-bond with Lys533. The consistent correlation between the in vitro activities of the ligands presented here (Table 1) and their respective interaction energy scores with the Top1/DNA complex (Table 2) give strong support to the docked orientations of the ligands in the Top1/DNA active site (Fig. 4, see Results and discussion).

A recent X-ray crystal structure of Top1 in irreversible covalent complex with a suicide-DNA contains topotecan, a CPT A-ring derivative, intercalated in the Top1/DNA active site between the +1 and −1 base pairs.[47] Staker et al. proposed that the E-ring opened topotecan carboxylate was important in inhibiting Top1 since they detected it in the X-ray crystal structure.[47] In contrast, our in vitro results have indicated that the hCPT carboxylate is inactive (Fig. 1) and that the hCPT β-hydroxylactone is stabilized by Top1 and DNA (Fig. 2, see Results and discussion). Interestingly, the same ratio of topotecan α-hydroxylactone–carboxylate (~70:30) was found in the Top1/suicide-DNA active site, as when topotecan was incubated in mother liquor alone.[47] This suggests that the crystallization conditions alone favored opening of the topotecan E-ring over time.

Interestingly, the suicide-DNA contains a backbone sulfur and cleavage of the suicide-DNA by Top1 results in a free 5′-SH on the cleavage-site +1 deoxynucleoside that cannot religate.[48] A 5′-SH would not form as strong electrostatic interactions with Arg488 and Asp533 as does the 5′OH in native DNA (Fig. 5B, see Results and discussion). A potential consequence is that Top1 may not hold the suicide-DNA +1 deoxynucleoside out of the helix as often, resulting in the loss of the inhibitor binding cavity described here (see Results and discussion). A second point is that topotecan does not block religation of the suicide-DNA,[48] and so the observed complex in the crystal may be different from a Top1/DNA complex where topotecan does block religation of the DNA. In the Top1/suicide-DNA/topotecan X-ray crystal structure the E-ring closed topotecan predominately interacts with the DNA via stacking interactions, while making only one H-bond to Top1.[47] In contrast, the biochemical evidence on ten reported Top1 resistance mutations to CPT and 10-OH CPT indicates numerous interactions between Top1 and inhibitor.[5,12]

Previously, we demonstrated that SN38 (CPT 10-OH, 7-ethyl), a potent Top1 inhibitor,[49–51] made a H-bond with Asn352, and that mutation of Asn352 to Ala resulted in Top1/Asn352Ala that was resistant to 10-OH derivatives of CPT to the same level as it was to CPT.[12] Here the molecular modeling results for hCPT 9,10 diF binding in the solvated Top1/DNA active site indicate that its increased potency is also due to it making a H-bond with Asn352.

Together these correlated experimental and computational results provide insight into the mechanism of hCPT and derivatives inhibition of Top1, while defining the atomic requirements of the E-ring, independently of E-ring opening. Furthermore, the Top1/DNA active-site model presented here can be tested since the orientation of hCPT 9,10 diF in the Top1/DNA active site indicates that more potent hCPT derivatives could be developed via engineered interactions with as yet unutilized Top1 active-site residues including: Glu356, Asn430 (not shown), and Lys751 (see Fig. 4A).

4. Experimental

4.1. Synthesis of hCPT and derivatives

The synthesis of all ligands has been reported.[29,30] The structures of all ligands were confirmed by NMR spectroscopy. hCPT ketone and hCPT 20-ketopropyl were racemic (all molecular modeling used the enantiomers shown in Table 1), while CPT was > 95% of the 20-*S* enantiomer. hCPT, hCPT 9,10 diF, and hCPT 10,11 diF were >95% of the 20-*R* enantiomer, these correspond to the biologically active configurations shown in Table 1.

4.2. Top1 expression and purification

The wild type (wt) Top1 construct is similar to that reported elsewhere.[52] Briefly, the wt Top1 gene was cloned into a baculovirus transfer vector and used to make a recombinant baculovirus following the manufacturer's recommendations (BD-PharMingen, San Diego, CA). The wt Top1 was then expressed in TN5 insect cells (HighFive, Invitrogen Corp., San Diego, CA) via the recombinant baculovirus, and purified via the N-terminal His tag essentially as described.[53,54]

4.3. End-labeling of oligonucleotides

Oligonucleotides were based on a high affinity tetrahymena rDNA Top1 cleavage site.[55,56] The single-stranded scissile-strand oligonucleotides were 3′-end-labeled with ^{32}P-cordycepin[11] to give either a 23-mer 5′-AAAAAGACTt/GGAAAAATTTTTA*-3′, or a 33-mer 5′-AAAAAGACTt/GAAACGTTTTACAACAATTAAAA*-3′ with / indicating the cleavage site, t indicating the −1 thymine to which the Top1 Tyr723 makes a covalent bond, and A* indicating the ^{32}P-cordycepin label. The oligonucleotides used in Section 4.5 (Fig. 1) were obtained commercially from MWG-Biotech (HPLC purified; High Point, NC), while the oligonucleotides used in Section 4.6 (Fig. 3) were from Oligosetc (PAGE purified; Wilsonville, OR). Oligonucleotides were annealed with a 5 M excess of unlabeled nonscissile-strand oligonucleotide to form dsDNA in either buffer 1 (Tris 10 mM pH 7.4, 100 mM NaCl, 1 mM EDTA) for the in vitro assays in Section 4.5, or buffer 2 (20 mM $NaPO_4$, 50 mM NaCl) for the guanine oxidation assays in Section 4.6, by heating for 4 min at 95 °C and then cooling at a linear rate from 90 to 24 °C in 60 min.

4.4. In vitro analysis of hCPT E-ring opening

In order to quantify the hCPT E-ring opening in vitro, hCPT (1 μM) was incubated at 24 °C in: (1) 50 mM CAPS pH 10.5, 0.1 mM DTT; (2) buffer 3 (10 mM Tris, pH 7.4, 50 mM NaCl, 5 mM $MgCl_2$, 0.1 mM DTT); and (3) buffer 3 and Top1 with an unlabeled 22-mer dsDNA (each at 2 μM, for dsDNA see Section 4.3). After 5 h, reactions were stopped by the addition SDS (0.5% final concentration) and centrifuged for 3 min at 3000*g*. An aliquot was then immediately analyzed by HPLC,[57] on a Zorbax Eclipse XDB C18 column 4.6 × 250 mm (Agilent Technologies Inc., Wilmington, DE), eluted at 1.2 mL/min with a linear gradient of acetonitrile in triethylammonium acetate buffer [2% (v/v), adjusted to pH 5.5] that increased the acetonitrile concentration from 20% to 35% over 15 min (Fig. 2). Experiments were done in replicates.

4.5. Top1 in vitro oligonucleotide assays

The end-labeled 23-mer dsDNA substrate (~10 nM, see Section 4.3) was incubated with Top1 (3 nM) either with or without the indicated ligand, for 20 min at 23 °C in buffer 3. Reactions were stopped by addition of SDS to 0.5%. To prepare the sample for electrophoresis, 3 volumes of loading buffer (98% formamide, 1 mg/mL xylene cyanol and 1 mg/mL bromophenol blue) were added to reaction mixtures. Twenty percent denaturing polyacrylamide gels (7 M urea) were run at 60 W for ~2 h. Imaging and quantification were performed using a PhosphorImager and ImageQuant software, respectively (Molecular Dynamics, Sunnyvale, CA).

4.6. Oxidation of extra-helical deoxyguanosines

Human topoisomerase I at 0.6 mg/mL in 50% glycerol, 12.5 mM Tris pH 7.4, 2.5 mM EDTA, and 2.5 mM DTT was first diluted 1/100 in buffer 2, and then 1/10 into the reaction (final Top1 concentration 8.8 nM) containing buffer 4 (20 mM $NaPO_4$, 50 mM NaCl, 5 mM $MgCl_2$) and 10 nM end-labeled 33-mer dsDNA. A 10 mM stock of hCPT in 100% DMSO was diluted 1/200 in buffer 2 and then 1/10 into the above reaction to give 5 μM hCPT. The 10 μL reaction was incubated at 23 °C for 15 min to allow Top1/DNA covalent complexes to be trapped by hCPT, after which $CoCl_2$ (Fisher Scientific Co., Pittsburgh, PA) was added at the indicated concentration followed by $KHSO_5$ at a 10-fold molar excess (OXONE®, Sigma-Aldrich, St. Louis, MO). The reactions were incubated for 5 additional min at 23 °C after which they were stopped by addition of EDTA (10 mM final), SDS (0.5% final), 1 μL of proteinase K (0.5 units) in 50% glycerol and then incubated at 23 °C for 5 min. Next, 5 volumes of ethanol and 40 μg of calf thymus tRNA were added. After incubation at −70 °C for 1 h, the samples were centrifuged at 13 g for 15 min. The supernatant was removed and the precipitated DNA/tRNA pellet was dried under vacuum. The pellet was then resuspended in 30 μL of 10% piperidine (Sigma-Aldrich, St. Louis, MO) and heated at 90 °C for 30 min, after which the samples were then lyophilized. The DNA/tRNA pellets were resuspended in 15 μL of H_2O and lyophilized again. The final DNA/tRNA pellets were then resuspended in loading buffer (98% formamide, 1 mg/mL xylene cyanol and 1 mg/mL bromophenol blue) and loaded onto 20% PAGE containing 7 M urea. Imaging and quantification were performed using a PhosphorImager and ImageQuant software, respectively (Molecular Dynamics, Sunnyvale, CA). The ssDNA, dsDNA, and Top1/dsDNA controls contained hCPT/Top1, hCPT/denatured Top1, and hCPT carboxylate, respectively. hCPT (10 mM) was diluted 1/10 into 10 μL of 50 mM NaOH and incubated for 10 min at 23 °C, after which 160 μL H_2O and 20 μL of 10X assay buffer 2 was added. Top1 was treated the same way. The use of PAGE purified oligonucleotides in this assay eliminated the nonspecific background bands seen in Figure 1B.

4.7. Molecular modeling: ligand preparation

Three-dimensional structures of the ligands (Table 1) were constructed using the Builder module in Insight II version 2000.1 (Accelrys, San Diego, CA), and hydrogens and bond order were then added. Next, atom potentials/partial charges were assigned by the CFF force field (Accelrys, San Diego, CA). Note: all ligand C-ring C15 and C16 atom potentials were manually corrected from cpb (bridge carbon biphenyl functional group) to cp (Sp2 aromatic carbon in either a five- or six-member ring). The geometry of the ligands were optimized using the nonbond cell multipole summation method within Insight II/Discover_3 (Accelrys, San Diego, CA).

4.8. Molecular modeling: Top1/DNA covalent complex preparation

The X-ray crystal structure of human topoisomerase I in covalent complex with suicide-DNA,[10] as prepared for molecular modeling in the following ways: (1) all

missing amino acid side chains were built in using the Biopolymer module in Insight II and the built-in residues near the active site were orientated similar to those in a more recent Top1 structure;[58] (2) all 5-iodo-deoxyuridines in the DNA were converted into thymines by replacing the 5-iodo with a C5 methyl, and then the bases were replaced with thymines; (3) the +1 scissile-strand thymine was replaced with a guanine while the complementary nonscissile-strand +1 adenine was replaced with a cytosine to create a high affinity Top1 cleavage site.[55] Top1 does not contact these bases when they are base paired;[10] (4) the suicide-DNA backbone sulfur atom, found at the 5′ end of the +1 scissile-strand dG, was replaced with the native oxygen; (5) hydrogens and bond order were added to the Top1/DNA covalent complex, and then atom potentials/partial charges were assigned using the CFF force field in Insight II. The following atoms′ bond order/potentials/partial charges were assigned manually using CFF force field parameters: the tyrosyl-phosphate bond atoms; the Tyr723 ring atoms/hydrogens; and as needed, the +1 dG, the −1 deoxythymidine, and the DNA strands' terminal atoms. The CFF force field (Accelrys, San Diego, CA) includes parameters for protein, nucleic acids, and small molecules.[59–61] (6) The +1 dG was rotated, via the backbone P–O bond, out of the helix until the free 5′-OH oxygen came within ~3 Å of Asp533; (7) hCPT 9,10 diF was manually docked into the Top1/DNA active site such that the E-ring 20-ethyl occupied the space vacated by the rotated +1 dG, and the inhibitor made a network of H-bond and electrostatic interactions with the following active site residues: Asn352, Arg364, Lys532, and Asn722; (8) In order to make the system electroneutral sodium and chloride counter ions were added to the Top1/DNA covalent complex; (9) The Top1/DNA/ligand complex was soaked with explicit waters until a 5 Å layer of water covered the Top1/DNA/ligand complex. The hydrogen atoms, waters, and ions were then minimized using the nonbond cell multipole summation method (Insight II/Discover_3); (10) Top1 residues Arg488, Asp533, Ile535, and Arg590 were then minimized to optimize their interactions with the rotated +1 dG; (11) The DNA/water/ions above hCPT 9,10 diF were then minimized with no restraints, resulting in the nonscissile-strand and scissile-strand deoxynucleosides moving up, to make room for the inhibitor. The Top1/DNA active site was soaked a second time with solvent and all water molecules in the system (WTR) were renamed H2O, so that the two water subsets could then be merged; (12) Active-site residues (excluding Tyr723 and the tyrosyl-phosphate bond to the −1 thymine), waters and ions were then minimized to optimize their interactions with hCPT 9,10 diF and the bound DNA. Molecular dynamics simulations were run using the Discover_3 module of Insight II to search for alternate orientations of ligand side groups and Top1 active-site residues.

4.9. Docking ligands into the Top1/DNA active site

Ligands were orientated such that they could make the maximum number of H-bonds/electrostatic interactions with active site residues and DNA including: Asn352, Arg364, Lys532, Asn722, and the −1 scissile-strand base. Ligands were initially docked in the same orientation as hCPT 9,10 diF in the Top1/DNA active site (see Section 4.8). Each ligand, the Top1/DNA active-site amino acid side chains, surrounding DNA (including the rotated +1 dG) and all waters/ions in the system were then minimized with no restraints in Discover_3 using the nonbond cell multipole summation method until a Final Convergence of 15 was reached. Next, waters within 20 Å of the ligand were minimized to a Final Convergence of 1. Finally, a minimization was run in which the ligand, active-site amino acid side chains, surrounding DNA (including the rotated +1 dG), and waters within 20 Å were then minimized with no restraints using the nonbond cell multipole summation method with a distance dependent dielectric until a Final Convergence of 1 was reached. The water/ions/DNA were then merged with Top1 and the interaction energy between each ligand and the solvated Top1/DNA covalent complex was calculated. For the interaction energy calculation between the +1 dG and Top1, the water/ions were first merged with Top1. All interaction energy calculations were done in the Docking module of Insight II and used the nonbond atom based summation method with a 20 Å cut off.

Acknowledgements

We dedicate this paper to the memory of Professor Thomas G. Burke, a pioneer in camptothecin research. We thank Drs. Marc Nicklaus, Rajeshri Karki, Steven Rokita, Cynthia Burrows, and James Muller for thoughtful discussions and advice, as well as Dr. Heiko Kroth for careful review of the manuscript. G.S.L. is supported by a National Cancer Institute postdoctoral fellowship, W.D. thanks the University of Pittsburgh for a Mellon Predoctoral Fellowship, and D.P.C. thanks the National Institutes of Health for their support.

References and notes

1. Champoux, J. In *DNA Topology and its Biological Effects*; Wang, J. C., Cozarelli, N. R., Eds.; Cold Spring Harbor Laboratory: Cold Spring Harbor, 1990; p 217.
2. Pommier, Y.; Tanizawa, A. In *Cancer Chemotherapy*; Hickman, J., Tritton, T., Eds.; Blackwell Scientific Publications Ltd: Oxford, 1993; p 214.
3. Chen, A. Y.; Liu, L. F. *Annu. Rev. Pharmacol. Toxicol.* **1994**, *94*, 194.
4. Pommier, Y. *Biochimie* **1998**, *80*, 255.
5. Pommier, Y.; Pourquier, P.; Urasaki, Y.; Wu, J.; Laco, G. S. *Drug Resist. Updates* **1999**, *2*, 307.
6. Wall, M. E.; Wani, M. C.; Cooke, C. E.; Palmer, K. H.; McPhail, A. T.; Slim, G. A. *J. Am. Chem. Soc.* **1966**, *88*, 3888.
7. Thomas, C. J.; Rahier, N. J.; Hecht, S. M. *Bioorg. Med. Chem.* **2004**, *12*, 1585.
8. Wang, J. C. *Annu. Rev. Biochem.* **1996**, *65*, 635.
9. Champoux, J. J. *Prog. Nucleic Acids Res. Mol. Biol.* **1998**, *60*, 111.
10. Redinbo, M. R.; Stewart, L.; Kuhn, P.; Champoux, J. J.; Hol, W. G. *Science* **1998**, *279*, 1504.

11. Pommier, Y.; Laco, G. S.; Kohlhagen, G.; Sayer, J. M.; Kroth, H.; Jerina, D. M. *Proc. Natl. Acad. Sci. U.S.A.* **2000**, *97*, 10739.
12. Laco, G. S.; Collins, J. R.; Luke, B. T.; Kroth, K.; Sayer, J. M.; Jerina, D. M.; Pommier, Y. *Biochemistry* **2002**, *41*, 1428.
13. Gromova, I. I.; Kjeldse, E.; Svejstrup, J. Q.; Alsner, J.; Christiansen, K.; Westergaard, O. *Nucleic Acids Res.* **1993**, *21*, 593.
14. Hsiang, Y. H.; Hertzberg, R.; Hecht, S.; Liu, L. F. *J. Biol. Chem.* **1985**, *260*, 14873.
15. Snapka, R. M.; Permana, P. A. *Bioessays* **1993**, *15*, 121.
16. Tsao, Y. P.; Russo, A.; Nyamusa, G.; Silber, R.; Liu, L. F. *Cancer Res.* **1993**, *53*, 5908.
17. Strumberg, D.; Pilon, A. A.; Smith, M.; Hickey, R.; Malkas, L.; Pommier, Y. *Mol. Cell Biol.* **2000**, *20*, 3977.
18. Holm, C.; Covey, J. M.; Kerrigan, D.; Pommier, Y. *Cancer Res.* **1989**, *49*, 6365.
19. Hsiang, Y.-H.; Lihou, M. G.; Liu, L. F. *Cancer Res.* **1989**, *49*, 5077.
20. Ryan, A. J.; Squires, S.; Strutt, H. L.; Johnson, R. T. *Nucleic Acids Res.* **1991**, *19*, 3295.
21. Mi, Z.; Burke, T. G. *Biochemistry* **1994**, *33*, 10325.
22. Yang, D.; Strode, J. T.; Spielmann, H. P.; Wang, A.; Burke, T. G. *J. Am. Chem. Soc.* **1998**, *120*, 2979.
23. Hertzberg, R. P.; Caranfa, M. J.; Hecht, S. M. *Biochemistry* **1989**, *28*, 4629.
24. Hsiang, Y.-H.; Liu, L. F.; Wall, M. E.; Wani, M. C.; Nicholas, A. W.; Manikumar, G.; Kirschenbaum, S.; Silber, R.; Potmesil, M. *Cancer Res.* **1989**, *49*, 4385.
25. Fassberg, J.; Stella, V. J. *J. Pharm. Sci.* **1992**, *81*, 676.
26. Burke, T. G.; Mi, Z. *Anal. Biochem.* **1993**, *212*, 285.
27. Burke, T. G.; Mi, Z. *J. Med. Chem.* **1993**, *36*, 2580.
28. Lavergne, O.; Lesuerur-Ginot, L.; Rodas, F. P.; Bigg, D. C. H. *Bioorg. Med. Chem. Lett.* **1997**, *7*, 2235.
29. Garbarda, A. E.; Du, W.; Isarno, T.; Tangirala, R. S.; Curran, D. P. *Tetrahedron* **2002**, *58*, 6329.
30. Du, W.; Curran, D. P.; Bevins, R. L.; Zimmer, S. G.; Zhang, J.; Burke, T. G. *Bioorg. Med. Chem. Lett.* **2002**, *10*, 103.
31. Yamazaki, T.; Kitazume, T. In *Enantiocontrolled Synthesis of Fluoro-Organic Compounds*; Soloshonok, V. A., Ed.; John Wiley & Sons, Ltd: New York, 1999; p 582.
32. Warshel, A.; Papazyan, A.; Kollman, P. A. *Science* **1995**, *269*, 102.
33. Muller, J. G.; Chen, X.; Dadiz, A. C.; Rokita, S. E.; Burrows, C. J. *J. Am. Chem. Soc.* **1992**, *114*, 6407.
34. Muller, J. G.; Zheng, P.; Rokita, S. E.; Burrows, C. J. *J. Am. Chem. Soc.* **1996**, *118*, 2320.
35. Jaxel, C.; Kohn, K. W.; Wani, M. C.; Wall, M. E.; Pommier, Y. *Cancer Res.* **1989**, *49*, 1465.
36. Bailly, C.; Lansiaux, A.; Dassonneville, L.; Demarquay, D.; Coulomb, H.; Huchet, M.; Lavergne, O.; Bigg, D. C. *Biochemistry* **1999**, *38*, 15556.
37. Tanizawa, A.; Kohn, K. W.; Kohlhagen, G.; Leteurtre, F.; Pommier, Y. *Biochemistry* **1995**, *34*, 7200.
38. Fujimori, A.; Harker, W. G.; Kohlhagen, G.; Hoki, Y.; Pommier, Y. *Cancer Res.* **1995**, *55*, 1339.
39. Nicholas, A. W.; Wani, M. C.; Manikumar, G.; Wall, M. E.; Kohn, K. W.; Pommier, Y. *J. Med. Chem.* **1990**, *33*, 972.
40. Urasaki, Y.; Laco, G. S.; Pourquier, P.; Takebayashi, Y.; Kohlhagen, G.; Gioffre, C.; Zhang, H.; Chatterjee, D.; Pantazis, P.; Pommier, Y. *Cancer Res.* **2001**, *61*, 1964.
41. Wang, X.; Zhou, X.; Hecht, S. M. *Biochemistry* **1999**, *38*, 4374.
42. Chillemi, G.; Fiorani, P.; Benedetti, P.; Desideri, A. *Nucleic Acids Res.* **2003**, *31*, 1525.
43. Pourquier, P.; Ueng, L. M.; Fertala, J.; Wang, D.; Park, H. J.; Essigmann, J. M.; Bjornsti, M. A.; Pommier, Y. *J. Biol. Chem.* **1999**, *274*, 8516.
44. Andoh, T.; Ishii, K.; Suzuki, Y.; Ikegami, Y.; Kusunoki, Y.; Takemoto, Y.; Okada, K. *Proc. Natl. Acad. Sci. U.S.A.* **1987**, *84*, 5565.
45. Hautefaye, P.; Cimetiere, B.; Pierre, A.; Leonce, S.; Hickman, J.; Laine, W.; Bailly, C.; Lavielle, G. *Bioorg. Med. Chem. Lett.* **2003**, *13*, 2731.
46. Cagir, A.; Jones, S. H.; Gao, R.; Eisenhauer, B. M.; Hecht, S. M. *J. Am. Chem. Soc.* **2003**, *125*, 13628.
47. Staker, B. L.; Hjerrild, K.; Feese, M. D.; Behnke, C. A.; Burgin, A. B., Jr.; Stewart, L. *Proc. Natl. Acad. Sci.* **2002**, *99*, 15387.
48. Burgin, A. B., Jr.; Huizenga, B. N.; Nash, H. A. *Nucleic Acids Res.* **1995**, *23*, 2973.
49. Kaneda, N.; Nagata, H.; Furuta, T.; Yokokura, T. *Cancer Res.* **1990**, *50*, 1715.
50. Kawato, Y.; Aonuma, M.; Hirota, Y.; Kuga, H.; Sato, K. *Cancer Res.* **1991**, *51*, 4187.
51. Tanizawa, A.; Fujimori, A.; Fujimori, Y.; Pommier, Y. *J. Natl. Cancer Inst.* **1994**, *86*, 836.
52. Pourquier, P.; Takebayashi, Y.; Urasaki, Y.; Gioffre, C.; Kohlhagen, G.; Pommier, Y. *Proc. Natl. Acad. Sci. U.S.A.* **2000**, *97*, 1885.
53. Zhelkovsky, A. M.; Moore, C. L.; Rattner, J. B.; Hendzel, M. J.; Furbee, C. S.; Muller, M. T.; Bazett-Jones, D. P. *Protein Express. Purif.* **1994**, *5*, 364.
54. Pourquier, P.; Pilon, A. A.; Kohlhagen, G.; Mazumder, A.; Sharma, A.; Pommier, Y. *J. Biol. Chem.* **1997**, *272*, 26441.
55. Bonven, B. J.; Gocke, E.; Westergaard, O. *Cell* **1985**, *41*, 541.
56. Pourquier, P.; Ueng, L. M.; Kohlhagen, G.; Mazumder, A.; Gupta, M.; Kohn, K. W.; Pommier, Y. *J. Biol. Chem.* **1997**, *272*, 7792.
57. Warner, D. L.; Burke, T. G. *J. Chromatogr. B: Biomed. Sci. Appl.* **1997**, *691*, 161.
58. Redinbo, M. R.; Stewart, L.; Champoux, J. J.; Hol, W. G. *J. Mol. Biol.* **1999**, *292*, 685.
59. Hwang, M. J.; Ni, X.; Waldman, M.; Ewig, C. S.; Hagler, A. T. *Biopolymers* **1998**, *45*, 435.
60. Maple, J. R.; Hwang, M. J.; Jalkanen, K. J.; Stochfisch, T. P.; Hagler, A. T. *J. Comput. Chem.* **1998**, *19*, 430.
61. Ewig, C. S.; Berry, R.; Dinur, U.; Hill, J. R.; Hwang, M. J.; Li, H.; Liang, C.; Maple, J.; Peng, Z.; Stockfisch, T. P.; Thacher, T. S.; Yan, L.; Ni, X.; Hagler, A. T. *J. Comput. Chem.* **2001**, *22*, 1782.